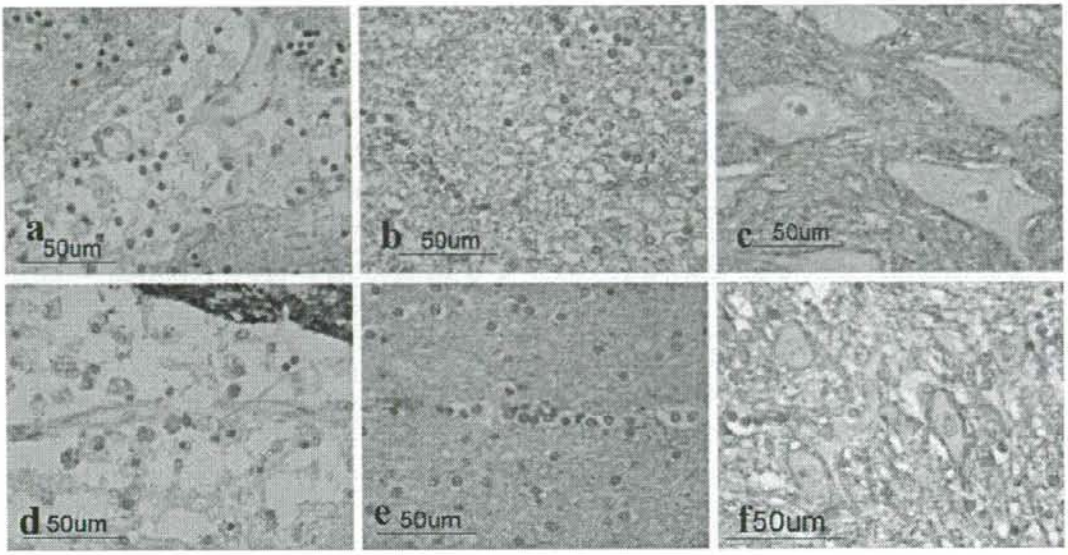

Fig. 7 Absence of aquaporin (AQP1 and AQP4) immunoreactivities in macrophages, neurons and oligodendrocyte cell bodies in multiple sclerosis (MS) and other neurological and psychiatric disease brains. The expression of AQP1 and AQP4 proteins was studied in MS patients, numbered from MS1 to MS4, and non-MS brains, numbered according to their disease, by immunohistochemistry. Panel (a) AQP1 (H-55), numerous perivascular macrophages in a chronic active demyelinating lesion in the frontal cerebral cortex of MS3; (b) AQP1 (H-55), surviving oligodendrocytes in a chronic active demyelinating lesion in the frontal cerebral cortex of MS2; (c) AQP1 (H-55), motor neurons in the spinal cord of MS2; (d) AQP4 (H-80), foamy macrophages in an acute necrotic lesion of a cerebral infarction in the parietal cerebral cortex of an 84-year-old man; (e) AQP4 (H-80), surviving oligodendrocytes in a chronic active demyelinating lesion in the parietal cerebral cortex of MS4; (f) AQP4 (H-80), pontine neurons in the brain stem of MS2.

immunoreactivity is not evident in areas of microvascular proliferation.[28-30] The robust expression of AQP on astroglial lineage cells suggests their involvement in the development of tumor-associated brain edema caused by a disruption of local water transport. Importantly, AQP1-null mice show reduced tumor vascularity and tumor cell migration after subcutaneous or intracranial implantation of tumor cells.[31] By contrast, the over-expression of AQP1 in NIH-3T3 cells accelerates anchorage-independent cell growth characteristic of malignant transformation.[32] Mammary gland tumor cells expressing the AQP1 transgene show increased tumor cell extravasation.[33] Glial scar formation following a cortical stab injury is remarkably impaired in AQP4-null mice associated with a reduced migration capacity of reactive astrocytes towards the site of injury.[34] All these observations suggest that both AQP1 and AQP4 play a fundamental role in cell growth and migration, possibly by a mechanism that involves cytoskeletal reorganization triggered by AQP-mediated water transport at the leading edge of the lamellipodia of proliferating and migrating cells. Furthermore, AQP1 plays a role in apoptotic cell shrinkage and affects downstream apoptotic events by regulating the cell volume.[35] By immunohistochemistry, we found that AQP1 was expressed not only on the plasma membrane but also in the cytoplasm and the nuclear membrane of cultured human astrocytes. The intracellular location of AQP1 has been reported previously. AQP1 integrates into the endoplasmic reticulum (ER) membrane when over-expressed in HEK293 cells.[36] Secretin induces a redistribution of AQP1 protein from intracellular vesicles to the cell plasma membrane in cholangiocytes.[37]

The regulatory mechanisms underlying AQP gene expression appear to be complex. Systemic hyponatremia elevates the levels of expression of AQP1 on CPE.[38] The induction of severe hydrocephalus up-regulates AQP4 but not AQP1 in perivascular astrocytes.[39] Pregnancy up-regulates AQP4 expression in rat brain tissues.[40] Treatment with corticosteroids increases AQP1 expression in the capillary endothelium of the peritoneal membrane and the lung.[41,42] Hypertonic stress induces the expression of AQP1 in rodent renal medullary cells by activating extracellular signal-regulated kinase, p38 mitogen-activated protein (MAP) kinase and c-Jun N-terminal kinase, all of which regulate a hypertonicity-responsive element located in the AQP1 promoter.[43] Testosterone up-regulates but phorbol

esters down-regulate AQP4 mRNA and protein levels in rodent astrocytes in culture.[44,45] The levels of AQP4 mRNA expression are elevated during the astrocytic differentiation of P19 embryonic carcinoma cells.[46] Interferon-alpha up-regulates AQP5 gene expression in human parotid acinar cells.[47] We for the first time showed that AQP4 levels were elevated markedly in human astrocytes by exposure to IFNγ, the prototype of T helper type-1 (Th1) cytokines, but neither by TNFα nor IL-1β, whereas AQP1 levels were unaffected by all these cytokines, although the IFN-responsive elements have not been identified in the promoter of the human AQP4 gene.[48]

It is worth noting that various human cell lines of neuronal origin, such as NTera2N, Y79, SK-N-SH and IMR-32, express substantial levels of AQP1 and AQP4 mRNA. Several previous studies showed that defined populations of neurons, along with neural stem cells, express AQP4 and/or AQP1 *in vivo*,[9,49-52] suggesting the possibility that these AQP play an active role in the maintenance of the water balance in a much broader spectrum of cell types in the CNS under physiological and pathological conditions.

In conclusion, the expression not only of AQP4 but also of AQP1 was identified in human astrocytes *in vitro* and *in vivo* in various neurological diseases including MS, suggesting a pivotal role of astrocytic AQP in regulation of water homeostasis in the human CNS under pathological conditions.

ACKNOWLEDGMENTS

This work was supported by grants to J. I. S. from Research on Psychiatric and Neurological Diseases and Mental Health, the Ministry of Health, Labour and Welfare of Japan (H17-kokoro-020), Research on Health Sciences Focusing on Drug Innovation, the Japan Health Sciences Foundation (KH21101) and a Grant-in-Aid for Scientific Research from the Ministry of Education, Culture, Sports, Science and Technology, Japan (B18300118). All autopsied the brain samples were obtained from the Research Resource Network, Japan.

REFERENCES

1. Agre P, King LS, Yasui M *et al.* Aquaporin water channels. From atomic structure to clinical medicine. *J Physiol* 2002; **542**: 3–16.
2. Verkman AS. More than just water channels: unexpected cellular roles of aquaporins. *J Cell Sci* 2005; **118**: 3225–32.
3. Nielsen S, Smith BL, Christensen EI, Agre P. Distribution of the aquaporin CHIP in secretory and resorptive epithelia and capillary endothelia. *Proc Natl Acad Sci USA* 1993; **90**: 7275–9.
4. Boassa D, Stamer WD, Yool AJ. Ion channel function of aquaporin-1 natively expressed in choroid plexus. *J Neurosci* 2006; **26**: 7811–19.
5. King LS, Choi M, Fernandez PC, Cartron JP, Agre P. Defective urinary concentrating ability due to a complete deficiency of aquaporin-1. *N Engl J Med* 2001; **345**: 175–9.
6. King LS, Nielsen S, Agre P, Brown RH. Decreased pulmonary vascular permeability in aquaporin-1-null humans. *Proc Natl Acad Sci USA* 2002; **99**: 1059–63.
7. Oshio K, Watanabe H, Song Y, Verkman AS, Manley GT. Reduced cerebrospinal fluid production and intracranial pressure in mice lacking choroid plexus water channel aquaporin-1. *FASEB J* 2005; **19**: 76–8.
8. Dolman D, Drndarski S, Abbott NJ, Rattray M. Induction of aquaporin 1 but not aquaporin 4 messenger RNA in rat primary brain microvessel endothelial cells in culture. *J Neurochem* 2005; **93**: 825–33.
9. Jung JS, Bhat RV, Preston GM, Guggino WB, Baraban JM, Agre P. Molecular characterization of an aquaporin cDNA from brain: candidate osmoreceptor and regulator of water balance. *Proc Natl Acad Sci USA* 1994; **91**: 13052–6.
10. Nielsen S, Nagelhus EA, Amiry-Moghaddam M, Bourque C, Agre P, Ottersen OP. Specialized membrane domains for water transport in glial cells: high-resolution immunogold cytochemistry of aquaporin-4 in rat brain. *J Neurosci* 1997; **17**: 171–80.
11. Amiry-Moghaddam M, Otsuka T, Hurn PD *et al.* An α-syntrophin-dependent pool of AQP4 in astroglial end-feet confers bidirectional water flow between blood and brain. *Proc Natl Acad Sci USA* 2003; **100**: 2106–11.
12. Manley GT, Fujimura M, Ma T *et al.* Aquaporin-4 deletion in mice reduces brain edema after acute water intoxication and ischemic stroke. *Nat Med* 2000; **6**: 159–63.
13. Papadopoulos MC, Verkman AS. Aquaporin-4 gene disruption in mice reduces brain swelling and mortality in pneumococcal meningitis. *J Biol Chem* 1995; **280**: 13906–12.
14. Solenov E, Watanabe H, Manley GT, Verkman AS. Sevenfold-reduced osmotic water permeability in primary astrocyte cultures from AQP-4-deficient mice, measured by a fluorescence quenching method. *Am J Physiol Cell Physiol* 2004; **286**: C426–C432.
15. Aoki K, Uchihara T, Tsuchiya K, Nakamura A, Ikeda K, Wakayama Y. Enhanced expression of aquaporin 4 in human brain with infarction. *Acta Neurpathol* 2003; **106**: 121–4.
16. Aoki-Yoshino K, Uchihara T, Duyckaerts C, Nakamura A, Hauw JJ, Wakayama Y. Enhanced expression

of aquaporin 4 in human brain with inflammatory diseases. *Acta Neuropathol* 2005; **110**: 281–8.
17. Lennon VA, Kryzer TJ, Pittock SJ, Verkman AS, Hinson SR. IgG marker of optic-spinal multiple sclerosis binds to the aquaporin-4 water channel. *J Exp Med* 2005; **202**: 473–7.
18. Binder DK, Oshio K, Ma T, Verkman AS, Manley GT. Increased seizure threshold in mice lacking aquaporin-4 water channels. *Neuroreport* 2004; **15**: 259–62.
19. Eid T, Lee TSW, Thomas MJ *et al.* Loss of perivascular aquaporin 4 may underlie deficient water and K^+ homeostasis in the human epileptogenic hippocampus. *Proc Natl Acad Sci USA* 2005; **102**: 1193–8.
20. Badaut J, Hirt L, Granziera C, Bogousslavsky J, Magistretti PJ, Regli L. Astrocyte-specific expression of aquaporin-9 in mouse brain is increased after transient focal cerebral ischemia. *J Cereb Blood Flow Metab* 2001; **21**: 477–82.
21. Satoh J, Yamamura T, Arima K. The 14-3-3 protein ε isoform expressed in reactive astrocytes in demyelinating lesions of multiple sclerosis binds to vimentin and glial fibrillary acidic protein in cultured human astrocytes. *Am J Pathol* 2004; **165**: 577–92.
22. Satoh J, Kuroda Y. Cytokines and neurotrophic factors fail to affect Nogo-A mRNA expression in differentiated human neurones: implications for inflammation-related axonal regeneration in the central nervous system. *Neuropathol Appl Neurobiol* 2002; **28**: 95–106.
23. Hoek AN van, Wiener MC, Verbavatz JM *et al.* Purification and structure. Functional analysis of native, PNGase F-treated, and endo-β-galactosidase-treated CHIP28 water channels. *Biochemistry* 1995; **34**: 2212–19.
24. Korolainen MA, Auriola S, Nyman TA, Alafuzoff I, Pirttilä T. Proteomic analysis of glial fibrillary acidic protein in Alzheimer's disease and aging brain. *Neurobiol Dis* 2005; **20**: 858–70.
25. Badaut J, Brunet JF, Grollimund L *et al.* Aquaporin 1 and aquaporin 4 expression in human brain after subarachnoid hemorrhage and in peritumoral tissue. *Acta Neurochir Suppl* 2003; **86**: 495–8.
26. Suzuki R, Okuda M, Asai J *et al.* Astrocytes co-express aquaporin-1-4, and vascular endothelial growth factor in brain edema tissue associated with brain contusion. *Acta Neurochir Suppl* 2006; **96**: 398–401.
27. Rodríguez A, Pérez-Gracia E, Espinosa JC, Pumarola M, Torres JM, Ferrer I. Increased expression of water channel aquaporin 1 and aquaporin 4 in Creutzfeldt-Jakob disease and in bovine spongiform encephalopathy-infected bovine-PrP transgenic mice. *Acta Neuropathol* 2006; **112**: 573–85.
28. Saadoun S, Papadopoulos MC, Davies DC, Bell BA, Krishna S. Increased aquaporin 1 water channel expression in human brain tumours. *Br J Cancer* 2002; **87**: 621–37.
29. Saadoun S, Papadopoulos MC, Davies DC, Krishna S, Bell BA. Aquaporin-4 expression is increased in oedematous human brain tumors. *J Neurol Neurosurg Psychiatry* 2002; **72**: 262–5.
30. Oshio K, Binder DK, Liang Y, Bollwn A, Feuerstein B, Berger MS, Manley GT. Expression of the aquaporin-1 water channel in human glial tumors. *Neurosurgery* 2005; **56**: 375–81.
31. Saadoun S, Papadopoulos MC, Hara-Chikuma M, Verkman AS. Impairment of angiogenesis and cell migration by targeted aquaporin-1 gene disruption. *Nature* 2005; **434**: 786–92.
32. Hoque MO, Soria JC, Woo J *et al.* Aquaporin 1 is overexpressed in lung cancer and stimulates NIH-3T3 cell proliferation and anchorage-independent growth. *Am J Pathol* 2006; **168**: 1345–53.
33. Hu J, Verkman AS. Increased migration and metastatic potential of tumor cells expressing aquaporin water channels. *FASEB J* 2006; **20**: 1892–4.
34. Saadoun S, Papadopoulos MC, Watanebe H, Yan D, Manley GT, Verkman AS. Involvement of aquaporin-4 in astroglial cell migration and glial scar formation. *J Cell Sci* 2005; **118**: 5691–8.
35. Jablonski EM, Webb AN, McConnell NA, Riley MC, Hughes FM Jr. Plasma membrane aquaporin activity can affect the rate of apoptosis but is inhibited after apoptotic volume decrease. *Am J Physiol Cell Physiol* 2004; **286**: C975–C985.
36. Dohke Y, Turner RJ. Evidence that the transmembrane biogenesis of aquaporin 1 is cotranslational in intact mammalian cells. *J Biol Chem* 2002; **277**: 15215–19.
37. Marinelli RA, Pham L, Agre P, LaRusso NF. Secretin promotes osmotic water transport in rat cholangiocytes by increasing aquaporin-1 water channels in plasma membrane. *J Biol Chem* 1997; **272**: 12984–8.
38. Moon Y, Hong SJ, Shin D, Jung Y. Increased aquaporin-1 expression in choroid plexus epithelium after systemic hyponatremia. *Neurosci Lett* 2006; **395**: 1–6.
39. Mao X, Enno TL, Del Bigio MR. Aquaporin 4 changes in rat brain with severe hydrocephalus. *Eur J Neurosci* 2006; **23**: 2929–36.
40. Quick AM, Cipolla MJ. Pregnancy-induced upregulation of aquaporin-4 protein in brain and its role in eclampsia. *FASEB J* 2005; **19**: 170–5.
41. King LS, Nielsen S, Agre P. Aquaporin-1 water channel protein in lung. Ontogeny, steroid-induced expression, and distribution in rat. *J Clin Invest* 1996; **97**: 2183–91.
42. Stoenoiu MS, Ni J, Verkaeren C *et al.* Corticosteroids induce expression of aquaporin-1 and increase trans-

cellular water transport in rat epithelium. *J Am Soc Nephrol* 2003; **14**: 555–65.
43. Umenishi F, Schrier RW. Hypertonicity-induced aquaporin-1 (AQP1) expression is mediated by the activation of MAPK pathways and hypertonicity-responsive element in the AQP1 gene. *J Biol Chem* 2003; **278**: 15765–70.
44. Yamamoto N, Sobue K, Miyachi T *et al.* Differential regulation of aquaporin expression in astrocytes by protein kinase C. *Mol Brain Res* 2001; **95**: 110–16.
45. Gu F, Hata R, Toku K *et al.* Testosterone up-regulates aquaporin-4 expression in cultured astrocytes. *J Neurosci Res* 2003; **72**: 709–15.
46. Yoneda K, Yamamoto N, Asai K *et al.* Regulation of aquaporin-4 expression in astrocytes. *Mol Brain Res* 2001; **89**: 94–102.
47. Smith JK, Siddiqui AA, Modica LA *et al.* Interferon-alpha upregulates gene expression of aquaporin-5 in human parotid glands. *J Interferon Cytokine Res* 1999; **19**: 929–35.
48. Yang B, Ma T, Verkman AS. cDNA cloning, gene organization, and chromosomal localization of a human mercurial insensitive water channel. Evidence for distinct transcriptional units. *J Biol Chem* 1995; **270**: 22907–13.
49. Venero JL, Vizuete ML, Ilundáin AA, Machado A, Echevarria M, Cano J. Detailed localization of aquaporin-4 messenger RNA in the CNS: preferential expression in periventricular organs. *Neuroscience* 1999; **94**: 239–50.
50. Cavazzin C, Ferrari D, Facchetti F *et al.* Unique expression and localization of aquaporin-4 and aquaporin-9 in murine and human neural stem cells and in their glial progeny. *Glia* 2005; **53**: 167–81.
51. Iandiev I, Pannicke T, Reichel MB, Wiedemann P, Reichenbach A, Bringmann A. Expression of aquaporin-1 immunoreactivity by photoreceptor cells in the mouse retina. *Neurosci Lett* 2005; **388**: 96–9.
52. Kang TH, Choi YK, Kim IB, Oh SJ, Chun MH. Identification and characterization of an aquaporin 1 immunoreactive amacrine-type cell of the mouse retina. *J Comp Neurol* 2005; **488**: 352–67.

Disease Markers 25 (2008) 27–35
IOS Press

Molecular network analysis of T-cell transcriptome suggests aberrant regulation of gene expression by NF-κB as a biomarker for relapse of multiple sclerosis

Jun-ichi Satoh[a,b,*], Tamako Misawa[a], Hiroko Tabunoki[a] and Takashi Yamamura[b]
[a]*Department of Bioinformatics and Molecular Neuropathology, Meiji Pharmaceutical University, Japan*
[b]*Department of Immunology, National Institute of Neuroscience, NCNP, Japan*

Abstract. Molecular mechanisms responsible for acute relapse of multiple sclerosis (MS) remain currently unknown. The aim of this study is to identify the relapse-specific biomarker genes in T lymphocytes of relapsing-remitting MS (RRMS). Total RNA of $CD3^+$ T cells isolated from six RRMS patients taken at the peak of acute relapse and at the point of complete remission was processed for DNA microarray analysis. We identified a set of 43 differentially expressed genes (DEG) between acute relapse and complete remission. By using 43 DEG as a discriminator, hierarchical clustering separated the cluster of relapse from that of remission. The molecular network of 43 DEG investigated by KeyMolnet, a bioinformatics tool for analyzing molecular interaction on the curated knowledge database, showed the most significant relationship with aberrant regulation of gene expression by the nuclear factor-kappa B (NF-κB) in T cells during MS relapse. These results support the logical hypothesis that NF-κB plays a central role in triggering molecular events in T cells responsible for induction of acute relapse of MS, and suggest that aberrant gene regulation by NF-κB on T-cell transcriptome might serve as a molecular biomarker for monitoring the clinical disease activity of MS.

Keywords: KeyMolnet, multiple sclerosis, nuclear factor-kappa B, relapse, T cells

1. Introduction

Multiple sclerosis (MS) is an inflammatory demyelinating disease of the central nervous system (CNS) white matter mediated by an autoimmune process triggered by a complex interplay of both genetic and environmental factors [1]. The great majority of MS patients show a relapsing-remitting (RR) clinical course. Intravenous administration of interferon-gamma (IFNγ) to MS patients provoked acute relapses accompanied by activation of the systemic immune response, indicating a pivotal role of proinflammatory T helper type 1 (Th1) lymphocytes in the immunopathogenesis of RRMS [2]. More recent studies proposed the pathogenic role of Th17 lymphocytes in sustained tissue damage in MS [3]. Several studies showed an etiological implication of viral infections for induction of acute relapse of MS [4]. However, the involvement of any viruses in MS relapse is not fully validated. A recent study showed that a methylprednisolone pulse therapy immediately reduces the levels of activated p65 subunit of the nuclear factor-kappa B (NF-κB) in lymphocytes of MS patients, suggesting a key role of NF-κB in induction of acute relapse of MS [5]. Furthermore, IFNγ is identified as one of NF-κB target genes, while IFNβ treatment attenuates proinflammatory responses in T cells by inhibiting the NF-κB activity [6,

*Corresponding author: Prof. Dr. Jun-ichi Satoh, Department of Bioinformatics and Molecular Neuropathology, Meiji Pharmaceutical University, 2-522-1 Noshio, Kiyose, Tokyo 204-8588, Japan. Tel./Fax: +81 42 495 8678; E-mail: satoj@my-pharm.ac.jp.

ISSN 0278-0240/08/$17.00

7]. At present, the precise molecular mechanism underlying MS relapse remains almost unknown. If the molecular biomarkers for MS relapse are identified, we could predict the timing of relapses, being highly valuable to start the earliest preventive intervention.

DNA microarray technology is a novel approach that allows us to systematically monitor the expression of a large number of genes in disease-affected tissues and cells. It has given new insights into molecular mechanisms promoting the autoimmune process in MS, and has made it possible to identify biomarkers for monitoring the clinical outcome [8]. The comprehensive gene expression profiling of MS brain tissues and peripheral blood lymphocytes identified a battery of genes deregulated in MS, whose role has not been previously predicted in its pathogenesis [9–12]. By microarray analysis, we recently identified a set of interferon-responsive genes expressed in highly purified peripheral blood $CD3^+$ T cells of RRMS patients receiving treatment with interferon-beta (IFNβ) [13]. IFNβ immediately induces a burst of expression of chemokine genes with potential relevance to IFNβ-related early adverse effects in MS [14]. The majority of differentially expressed genes in $CD3^+$ T cells between untreated MS patients and healthy subjects were categorized into apoptosis signaling regulators [15]. Furthermore, we found that T-cell gene expression profiling classifies a heterogeneous population of Japanese MS patients into four distinct subgroups that differ in the disease activity and therapeutic response to IFNβ [16].

In the present study, to identify MS relapse-specific biomarker genes, we conducted DNA microarray analysis of peripheral blood $CD3^+$ T cells isolated from RRMS patients taken at the peak of acute relapse and at the point of complete remission of the identical patients. We focused highly purified $CD3^+$ T cells because autoreactive pathogenic and regulatory cells, which potentially play a major role in MS relapse and remission, might be enriched in this fraction. Since microarray analysis usually produces a large amount of gene expression data at one time, it is often difficult to find out the meaningful relationship between gene expression profile and biological implications from such a large quantity of available data. To overcome this difficulty, we have made a breakthrough to identify the molecular network most closely associated with DNA microarray data by a novel data-mining tool of bioinformatics named KeyMolnet.

2. Subjects and methods

2.1. Blood samples

The present study included 6 Japanese women presenting with clinically active RRMS, diagnosed by certified neurologists of Department of Neurology, Musashi Hospital, National Institute of Neuroscience, National Center of Neurology and Psychiatry (NCNP), according to the established criteria [17]. Written informed consent was obtained from all the patients. The Ethics Committee of NCNP approved the present study. The patients showed the mean age of 41 ± 12 years and the mean Expanded Disability Status Scale (EDSS) score of 1.8 ± 0.5 (Fig. 1). None of the patients received treatment with glatiramer acetate, mitoxantrone or other immunosuppressants at any time in the entire clinical course. None of them were given methylprednisolone or interferons at least for three weeks before the time point of blood sampling. Blood samples of individual patients taken at two time points were compared, one at the point of complete remission and the other at the peak of acute relapse, usually on the day of onset or one day after acute relapse, just before starting treatment with intravenous methylprednisolone pulse (IVMP) or oral administration of high dose prednisolone (Fig. 1). The comprehensive clinical and neuroradiological evaluation on each case satisfied characteristics of either relapse or remission of MS.

2.2. Microarray analysis

The present study utilized a custom microarray containing duplicate spots of 1,258 cDNA, which were carefully designed by excluding any cross-hybridization, generated by PCR, and immobilized on a poly-L-lysine-coated slide glass (Hitachi Life Science, Kawagoe, Saitama, Japan) [13–16]. The array contains well-annotated biologically important human genes of various functional classes, which cover a wide range of cytokines/growth factors and their receptors, apoptosis regulators, oncogenes, transcription factors, signal transducers, cell cycle regulators and housekeeping genes (see the reference [14] for the complete gene list).

Peripheral blood mononuclear cells (PBMC) were isolated from 30 ml of heparinized blood by centrifugation on a Ficoll density gradient. They were labeled with anti-CD3 antibody-coated magnetic microbeads (Miltenyi Biotec, Auburn, CA), and $CD3^+$ T cells were separated by AutoMACS (Miltenyi Biotec). The puri-

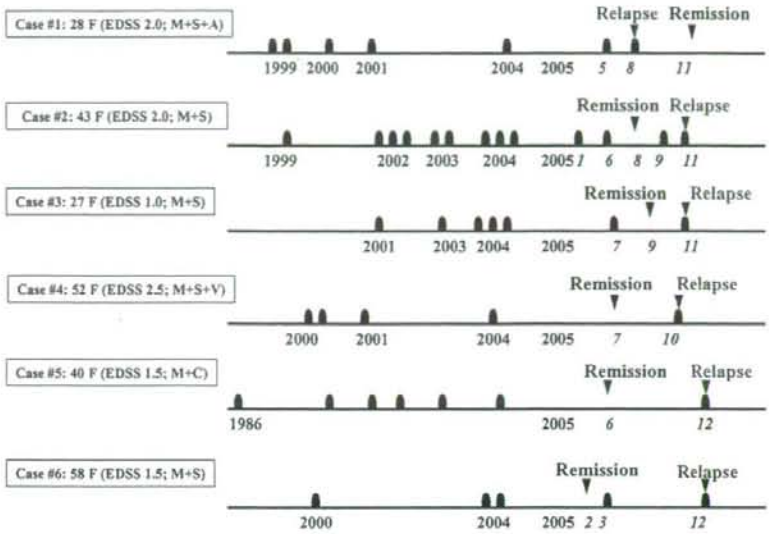

Fig. 1. Blood sampling from six RRMS patients in relapse and remission. Blood samples were taken from six patients with RRMS at the peak of acute relapse (red arrowhead) and at the time of complete remission (blue arrowhead). $CD3^+$ T cells were purified and processed for DNA microarray analysis. The relapses of MS (bell shape) specified by year and month (italic), age, sex, Expanded Disability Status Scale (EDSS) score, and cardinal clinical symptoms (M, motor impairment; S, sensory impairment; A, autonomic impairment; C, cognitive impairment; and V, visual impairment) are shown. The cases #3, 4, and 6 have a past history of short-term IFNβ treatment that was discontinued at the time point long enough to wash out the immunomodulatory effects of IFNβ on T-cell transcriptome.

ty of $CD3^+$ cells generally exceeded 90–95% by flow cytometric analysis. Total RNA was isolated from the cells by using RNeasy Mini Kit (Qiagen, Valencia, CA). Five μg of purified RNA was *in vitro* amplified, and the antisense RNA (aRNA) was labeled with a fluorescent dye Cy5, while universal reference aRNA was labeled with Cy3 to standardize the gene expression levels. The arrays were hybridized at 62 °C for 10 hours in the hybridization buffer containing equal amounts of Cy3- or Cy5-labeled cDNA, and they were then scanned by the ScanArray 5000 scanner (GSI Lumonics, Boston, MA). The data were analyzed by using the QuantArray software (GSI Lumonics). The average of fluorescence intensities (FI) of duplicate spots was obtained after global normalization between Cy3 and Cy5 signals. The gene expression level (GEL) was calculated according to the formula: GEL = FI (Cy5) of the sample/FI (Cy3) of the universal reference.

2.3. *Statistical analysis, hierarchical clustering, and molecular network analysis*

The genes differentially expressed between the samples of acute relapse and those of remission were identified by statistical evaluation with Student t-test via TTEST function of Excel, by comparing the log ratio of GEL of each gene at the two time points. The genes with a p value of < 0.05 were considered significant. Hierarchical clustering was performed on all the samples. The set of differentially expressed genes (DEG) was utilized as a discriminator to separate clusters following the "Gene Tree" algorithm on GeneSpring 7.2 (Agilent Technologies, Palo Alto, CA). This unsupervised approach arranged the genes and samples with a similar expression pattern to separate distinct clusters on the dendrogram.

The molecular network of DEG was analyzed by using a data-mining tool named KeyMolnet originally developed by the Institute of Medicinal Molecular Design, Inc. (IMMD), Tokyo, Japan [18], and the English version is currently utilized worldwide, including European Molecular Biology Laboratory (EMBL), Heidelberg, Germany (see the website of www.immd.co.jp/en/news/news20051222.html). KeyMolnet constitutes a knowledge-based content database of numerous interactions among human genes, molecules, diseases, pathways and drugs. They have been manually collected and carefully curated from selected review articles, literature, and public databases

by expert biologists of IMMD. The KeyMolnet contents, composed of approximately 12,000 molecules, are focused on human species, and categorized into either the core contents collected from selected review articles or the secondary contents extracted from abstracts of the PubMed database.

When the list of either GenBank accession number or probe ID of the genes extracted from microarray data was imported into KeyMolnet, it automatically provided corresponding molecules as a node on networks [18]. Among four different modes of the molecular network search, the "common upstream" search enables us to extract the most relevant molecular network composed of the genes coordinately regulated by putative "common upstream" transcription factors. The extracted molecular network was compared side by side with 346 distinct canonical pathways of human cells of the KeyMolnet library. They include a broad range of signal transduction pathways, metabolic pathways, and transcriptional regulations. The statistical significance in concordance between the extracted network and the canonical pathway was evaluated by the algorithm that counts the number of overlapping molecular relations between both. This makes it possible to identify the canonical pathway showing the most significant contribution to the extracted network. The calculation of significance score is based on the following formula, where O = the number of overlapping molecular relations between the extracted network and the canonical pathway, V = the number of molecular relations located in the extracted network, C = the number of molecular relations located in the canonical pathway, T = the number of total molecular relations installed in KeyMolnet, and X = the sigma variable that defines coincidence.

$$\text{Score} = -\log_2(\text{Score (p)})$$

$$\text{Score (p)} = \sum_{x=O}^{Min(C,V)} f(x)$$

$$\text{f(x)} = {}_{C}C_{x} \cdot {}_{T-C}C_{V-x} / {}_{T}C_{V}$$

3. Results

3.1. Microarray analysis identified 43 genes differentially expressed in peripheral blood T cells between relapse and remission of MS

Among 1,258 genes on the microarray, 43 genes were expressed differentially in peripheral blood $CD3^+$ T cells of 6 RRMS patients at the peak of acute relapse and at the point of complete remission (Table 1). Among 43 differentially expressed genes (DEG), 18 genes were upregulated, whereas 25 genes were downregulated at the time of relapse. Next, by using the set of 43 DEG as a discriminator, hierarchical clustering analysis was performed on total 12 samples, comprised of 6 relapse and 6 remission samples. Although the difference between the two groups was not so apparently huge, the clustering method effectively separated the cluster of relapse samples from the cluster of remission samples based on gene expression profile of 43 DEG, except for one remission sample included in the cluster of relapse samples (Fig. 2). These observations suggest that the gene network of signaling molecules located upstream of 43 DEG in T cells might be substantially different between two distinct clinical phases of MS.

3.2. Molecular network analysis suggests a key role of NF-κB in relapse of MS

To clarify the molecular network of 43 DEG regulated coordinately in T cells during acute relapse, their GenBank accession numbers and expression levels were imported into KeyMolnet. In the first step, GenBank accession numbers were converted into Keymolnet ID numbers. Then, the common upstream search of these generated a complex network composed of 128 fundamental nodes with 315 molecular relations. Among them, 25 nodes were included in the list of 43 DEG (Table 1), and 103 additional nodes outside the list were automatically incorporated from both core and secondary contents of KeyMolnet following the network-searching algorithm. The extracted molecular network was arranged with respect to subcellular location of the molecules by the editing function of KeyMolnet (Fig. 3). Finally, the statistical evaluation of the extracted network showed the most relevant relationship with transcriptional regulation by the nuclear factor NF-κB with the score of 11.036 and score (p) = 4.764E-004. No other canonical pathways (n = 345) than NF-κB-regulated gene transcription were identified as statistically significant in the extracted molecular network, judged by the scoring system involving the pathway based on molecular relations.

4. Discussion

To clarify molecular mechanisms underlying acute relapse of MS, we conducted DNA microarray analysis

Table 1
Fourty-three differentially expressed genes in T-cells between relapse and remission of MS

Rank	Gene symbol	KeyMolnet node	Full name	GenBank accession number	P value	Regulation in relapse versus remission
1	*PPARG*	PPARg	peroxisome proliferative activated receptor gamma	NM_005037	9.78E-04	up
2	*RND3*	Rnd3	Rho family GTPase 3	NM_005168	1.26E-03	down
3	*IL6*	IL-6	interleukin 6	NM_000600	1.97E-03	down
4	*AKT2*	AKT2	v-akt murine thymoma viral oncogene homolog 2	NM_001626	2.73E-03	up
5	*DCC*	DCC	deleted in colorectal carcinoma	NM_005215	3.80E-03	up
6	*CREBBP*	CBP	CREB binding protein	NM_004380	6.05E-03	down
7	*ATF5*	ATFx	activating transcription factor 5	NM_012068	6.99E-03	down
8	*PLCG1*	PLCg1	phospholipase C gamma 1	NM_002660	9.36E-03	up
9	*CDK3*	CDK3	cyclin-dependent kinase 3	NM_001258	1.01E-02	up
10	*RIPK1*	RIP1	receptor-interacting serine-threonine kinase 1	NM_003804	1.15E-02	up
11	*TNFRSF4*	OX40	TNF receptor superfamily, member 4	NM_003327	1.21E-02	down
12	*ABCC9*	SUR2	ATP-binding cassette, sub-family C, member 9	NM_005691	1.40E-02	down
13	*STAT2*	STAT2	signal transducer and activator of transcription 2	NM_005419	1.49E-02	up
14	*PTEN*	PTEN	phosphatase and tensin homolog	NM_000314	1.80E-02	down
15	*AVP*	AVP, VP, NPII, copeptin	arginine vasopressin	NM_000490	1.82E-02	up
16	*FADD*	FADD	Fas-associated via death domain	NM_003824	1.93E-02	up
17	*ELF2*	NERF2	E74-like factor 2 (ets domain transcription factor)	NM_006874	2.10E-02	down
18	*NFKB2*	p100NFkB, p52NFkB	NF-kappa B subunit 2 (p52/p100)	NM_002502	2.11E-02	up
19	*ERBB4*	Erb4, ERBB4	v-erb-a erythroblastic leukemia viral oncogene homolog 4	NM_005235	2.18E-02	down
20	*BCL2L1*	Bcl-XL	BCL2-like 1	NM_001191	2.53E-02	up
21	*BTRC*	b-TRCP, Fbw1	beta-transducin repeat containing protein	NM_003939	2.65E-02	up
22	*SULT1B1*	SULT1B1	sulfotransferase family, cytosolic, 1B, member 1	NM_014465	2.79E-02	down
23	*EP300*	p300	E1A binding protein p300	NM_001429	2.86E-02	down
24	*GJA4*	Cx37	gap junction protein alpha 4 (connexin 37)	NM_002060	2.87E-02	down
25	*PDGFB*	PDGF-B, PDGF-BB	platelet-derived growth factor beta polypeptie	NM_002608	2.92E-02	up
26	*ARID4A*	ARID4A	AT rich interactive domain 4A (RBP1-like)	NM_002892	3.05E-02	down
27	*CYP2C19*	CYP2C19	cytochrome P450, family 2, subfamily C, polypeptide 19	NM_000769	3.07E-02	down
28	*FGF1*	FGF-1	fibroblast growth factor 1	NM_000800	3.17E-02	down
29	*MMP2*	MMP-2	matrix metallopeptidase 2	NM_004530	3.27E-02	up
30	*ARHGAP1*	Cdc42GAP	Rho GTPase activating protein 1	NM_004308	3.35E-02	down
31	*TOP3B*	TOP3B	DNA topoisomerase III beta	NM_003935	3.97E-02	up
32	*SUB1*	PC4	SUB1 homolog	NM_006713	4.33E-02	down
33	*ZMYND8*	PRKCBP1	zinc finger, MYND-type containing 8	NM_183047	4.34E-02	down
34	*TGFB2*	TGFb2	transforming growth factor beta 2	NM_003238	4.36E-02	up
35	*SMAD7*	SMAD7	SMAD, mothers against DPP homolog 7	NM_005904	4.37E-02	down
36	*TCF4*	E2-2	transcription factor 4	NM_003199	4.40E-02	down
37	*NOS1*	nNOS	nitric oxide synthase 1 (neuronal)	NM_000620	4.42E-02	down
38	*TSC22D1*	TSC22	TSC22 domain family, member 1	NM_183422	4.54E-02	down
39	*GNB1L*	(none)	G protein beta subunit-like protein	NM_053004	4.57E-02	down
40	*IFNA8*	IFNA8	interferon alpha 8	NM_002170	4.60E-02	down
41	*IL1A*	IL-1a	interleukin 1 alpha	NM_000575	4.77E-02	up
42	*CD3D*	CD3d	CD3 delta	NM_000732	4.92E-02	up
43	*IL1R1*	IL-1R1	interleukin 1 receptor type I	NM_000877	4.95E-02	down

The genes differentially expressed between relapse and remission were identified by comparing the log ratio of gene expression level of each gene at two time points, evaluated by Student t-test. The genes with a p value of < 0.05 was selected. The gene symbol, KeyMolnet node name, full name, GenBank accession number, p value, and regulation in relapse versus remission are shown.

of peripheral blood $CD3^+$ T cells of 6 RRMS patients taken at the peak of acute relapse and at the point of complete remission of the identical patients. The battery of 43 genes was expressed differentially between relapse and remission. By using 43 DEG as a discriminator, hierarchical clustering analysis separated the cluster of relapse samples and the cluster consisting mainly of remission samples. Then, we for the first time intensively studied the molecular network of DEG between MS relapse and remission by using a bioinformatics tool for analyzing molecular interaction on the curated knowledge database named KeyMolnet. The common upstream search of 43 DEG on KeyMolnet indicated the central role of transcriptional regulation

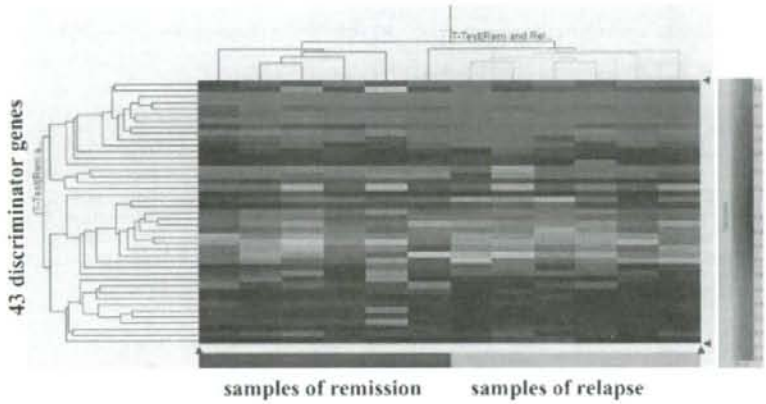

Fig. 2. Hierarchical clustering of 43 genes differentially expressed in T cells between relapse and remission of MS. Hierarchical clustering was performed on total 12 samples, consisting of 6 relapse (orange) and 6 remission (blue) samples, by using the set of 43 differentially expressed genes in T cells between relapse and remission (Table 1) as a discriminator. This separated two clusters, one composed of 5 remission samples and the other composed of 6 relapse samples and one remission sample. The matrix is labeled by a pseudo-color, with red expressing upregulation, green expressing downregulation, and the color intensity representing the magnitude of the deviation from GEL 1.0 as shown on the right.

by NF-κB in aberrant gene expression in T cells during MS relapse. We have recently characterized 286 genes differentially expressed in purified $CD3^+$ T cells between 72 untreated clinically-active MS patients and 22 age- and sex-matched healthy subjects [16]. When the set of 286 DEG was imported into KeyMolnet, the common upstream search illustrated the complex molecular network composed of 335 nodes. We found that the generated network showed again the most significant relationship with transcriptional regulation by NF-κB [19]. These observations, taken together, suggested that aberrant gene regulation by NF-κB on T-cell transcriptome might serve as a surrogate biomarker not only for discriminating MS from healthy subjects but also for monitoring the clinical disease activity of individual MS patients. This hypothesis warrants further evaluation by including a large cohort of MS patients whose blood samples are taken at acute relapse and during remission of the identical patients.

KeyMolnet stores the highly reliable content database of human proteins, small molecules, molecular relations, diseases, and drugs, carefully curated by experts from the literature and public databases [18]. This software makes it possible to effectively extract the most relevant molecular interaction from large quantities of gene expression data [19,20]. Our results indicate that the combination of DNA microarray and molecular network analysis is more effective to establish a biologically-relevant logical working model than the conventional microarray data analysis [21].

NF-κB is a central regulator of innate and adaptive immune responses, cell proliferation, and apoptosis [22,23]. The NF-κB family consists of five members, such as NF-κB1 (p50/p105), NF-κB2 (p52/p100), RelA (p65), RelB, and c-Rel. NF-κB exists in an inactive state in unstimulated cells, being sequestrated in the cytoplasm via non-covalent interaction with the inhibitor of NF-κB (IκB) proteins. Viral and bacterial products, cytokines, and stress-inducing agents activate specific IκB kinases that phosphorylate IκB proteins. Phosphorylated IκBs are ubiquitinated and processed for proteasome-mediated degradation, resulting in nuclear translocation of NF-κB that regulates the expression of target genes by binding to the consensus sequence located in the promoter.

Previous studies identified more than 150 NF-κB target genes, including those involved in not only immune, inflammatory and antiapoptotic responses, but also antiinflammatory and proapoptotic responses [24]. It is worthy to note that *BTRC*, β-transducin repeat containing protein, listed as one of upregulated genes in T cells of MS relapse (Table 1), acts as a RING E3 protein that mediates ubiquitination of IκBα [25]. Importantly, a number of NF-κB target genes activate NF-κB itself, providing a positive regulatory loop that amplifies and perpetuates inflammatory responses [22]. These observations raise the scenario that even subclinical levels of infections and stresses affecting the immune and neuroendocrine systems [4,26] could induce the persistent oscillation between activation and inactivation of

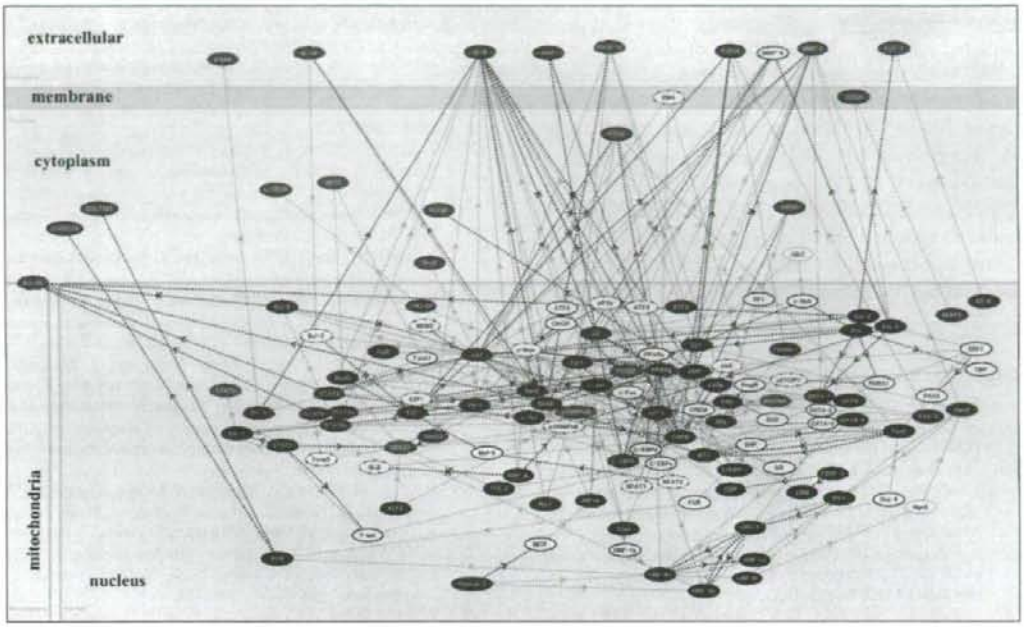

Fig. 3. The common upstream search of differentially expressed genes in T cells between relapse and remission of MS. The GenBank accession numbers and expression levels of 43 genes were imported into KeyMolnet. The "common upstream" search of these generated a network composed of 128 fundamental nodes with 315 molecular relations. It is shown with respect to subcellular location of molecules. Red nodes represent starting point molecules, whereas blue nodes represent common upstream molecules. Purple nodes express characteristics of both starting point and common upstream molecules. White nodes exhibit additional molecules extracted automatically from KeyMolnet core and secondary contents incorporated in the network to establish molecular connections. The direction of molecular relation is indicated by dash line with arrow (transcriptional activation) or dash line with arrow and stop (transcriptional repression). Thick lines indicate the core contents, while thin lines indicate the secondary contents of KeyMolnet. The statistical evaluation of the extracted molecular network indicated the principal relationship with transcriptional regulation by the nuclear factor NF-κB.

NF-κB in autoreactive T cells, thereby cause the fluctuation of disease activity from relapse to remission in RRMS patients. Unusual posttranslational modification of IκB and of NF-κB proteins occasionally causes aberrant NF-κB activation [27].

Increasing evidence supports a central role of aberrant NF-κB activation in development of MS. Pathologically, RelA, c-Rel, and p50 subunits of NF-κB are overexpressed in macrophages in active demyelinating lesions of MS [28], while RelA is activated in oligodendrocytes that survive in the lesion edge [29]. Geneticall-y, a predisposing allele in the NFKBIL gene is closely associated with development of RRMS [30]. We previously showed that the orphan nuclear receptor NR4A2, a direct target gene of NF-κB, is upregulated at the highest level in $CD3^+$ T cells of untreated MS patients [15, 16]. Targeted disruption of the NFKB1 gene confers resistance to development of experimental autoimmune encephalomyelitis (EAE), an animal model of MS [31]. *In vivo* administration of selective inhibitors of NF-κB protects mice from EAE [32]. Furthermore, the CNS-restricted inactivation of NF-κB ameliorates EAE, accompanied by a defect in induction of proinflammatory genes in astrocytes [33]. These results suggest that development of drugs aimed at fine-tuning of NF-κB function in T lymphocytes could provide a promising approach to suppress the clinical activity of MS.

In conclusion, the molecular network analysis of T-cell transcriptome suggests the logical hypothesis that abnormal transcriptional regulation by NF-κB plays a central role in aberrant gene expression in T cells during MS relapse, and that aberrant gene regulation by NF-κB on T-cell transcriptome might serve as a molecular biomarker for monitoring the clinical disease activity of individual MS patients. Although the study population (n = 6) is relatively small, our observations warrant further evaluation by using a large cohort of RRMS patients.

Acknowledgements

This work was supported by grants to J-IS from Research on Psychiatric and Neurological Diseases and Mental Health, the Ministry of Health, Labour and Welfare of Japan (H17-020), Research on Health Sciences Focusing on Drug Innovation, the Japan Health Sciences Foundation (KH21101), the Grant-in-Aid for Scientific Research, the Ministry of Education, Culture, Sports, Science and Technology, Japan (B18300118), and from the Nakatomi Foundation.

References

[1] A. Compston and A. Coles, Multiple sclerosis, *Lancet* **359** (2002), 1221–1231.

[2] H.S. Panitch, R.L. Hirsch, J. Schindler and K.P. Johnson, Treatment of multiple sclerosis with gamma interferon: Exacerbations associated with activation of the immune function, *Neurology* **37** (1987), 1097–1102.

[3] L. Steinman, A brief history of T_H17, the first major revision in the T_H1/T_H2 hypothesis of T cell-mediated tissue damage, *Nat Med* **13** (2007), 139–145.

[4] D. Buljevac, H.Z. Flach, W.C.J. Hop, D. Hijdra, J.D. Laman, H.F.J. Savelkoul, F.G.A. van der Meché, P.A. van Doorn and R.Q. Hintzen, Prospective study on the relationship between infections and multiple sclerosis exacerbations, *Brain* **125** (2002), 952–960.

[5] M. Eggert, R. Goertsches, U. Seeck, S. Dilk, G. Neeck and U.K. Zettl, Changes in the activation level of NF-kappa B in lymphocytes of MS patients during glucocorticoid pulse therapy, *J Neurol Sci* **264** (2008), 145–150.

[6] A. Sica, L. Dorman, V. Viggiano, M. Cippitelli, P. Ghosh, N. Rice and H.A. Young, Interaction of NF-κB and NFAT with the interferon-γ promoter, *J Biol Chem* **272** (1997), 30412–30420.

[7] F.M. Martín-Saavedra, N. Flores, B. Dorado, C. Eguiluz, B. Bravo, A. García-Merino and S. Ballester, Beta-interferon unbalances the peripheral T cell proinflammatory response in experimental autoimmune encephalomyelitis, *Mol Immunol* **44** (2007), 3597–3607.

[8] R. Goertsches, P. Serrano-Fernández, S. Møller, D. Koczan and U.K. Zettl, Multiple sclerosis therapy monitoring based on gene expression, *Curr Pharm Des* **12** (2006), 3761–3779.

[9] C. Lock, G. Hermans, R. Pedotti, A. Brendolan, E. Schadt, H. Garren, A. Langer-Gould, S. Strober, B. Cannella, J. Allard, P. Klonowski, A. Austin, N. Lad, N. Kaminski, S.J. Galli, J.R. Oksenberg, C.S. Raine, R. Heller and L. Steinman, Gene-microarray analysis of multiple sclerosis lesions yields new targets validated in autoimmune encephalomyelitis, *Nat Med* **8** (2002), 500–508.

[10] U. Graumann, R. Reynolds, A.J. Steck and N. Schaeren-Wiemers, Molecular changes in normal appearing white matter in multiple sclerosis are characteristic of neuroprotective mechanisms against hypoxic insult, *Brain Pathol* **13** (2003), 554–573.

[11] S. Stürzbecher, K.P. Wandinger, A. Rosenwald, M. Sathyamoorthy, A. Tzou, P. Mattar, J.A. Frank, L. Staudt, R. Martin and H.F. McFarland, Expression profiling identifies responder and non-responder phenotypes to interferon-β in multiple sclerosis, *Brain* **126** (2003), 1219–1429.

[12] A. Achiron, M. Gurevich, N. Friedman, N. Kaminski and M. Mandel, Blood transcriptional signatures of multiple sclerosis: unique gene expression of disease activity, *Ann Neurol* **55** (2004), 410–417.

[13] F. Koike, J. Satoh, S. Miyake, T. Yamamoto, M. Kawai, S. Kikuchi, K. Nomura, K. Yokoyama, K. Ota, T. Kanda, T. Fukazawa and T Yamamura, Microarray analysis identifies interferon β-regulated genes in multiple sclerosis, *J Neuroimmunol* **139** (2003), 109–118.

[14] J. Satoh, Y. Nanri, H. Tabunoki and T. Yamamura, Microarray analysis identifies a set of CXCR3 and CCR2 ligand chemokines as early IFNβ-responsive genes in peripheral blood lymphocytes: an implication for IFNβ-related adverse effects in multiple sclerosis, *BMC Neurol* **6** (2006), 18.

[15] J. Satoh, M. Nakanishi, F. Koike, S. Miyake, T. Yamamoto, M. Kawai, S. Kikuchi, K. Nomura, K. Yokoyama, K. Ota, T. Kanda, T. Fukazawa and T. Yamamura, Microarray analysis identifies an aberrant expression of apoptosis and DNA damage-regulatory genes in multiple sclerosis, *Neurobiol Dis* **18** (2005), 537–550.

[16] J. Satoh, M. Nakanishi, F. Koike, H. Onoue, T. Aranami, T. Yamamoto, M. Kawai, S. Kikuchi, K. Nomura, K. Yokoyama, K. Ota, T. Saito, M. Ohta, S. Miyake, T. Kanda, T. Fukazawa and T. Yamamura, T cell gene expression profiling identifies distinct subgroups of Japanese multiple sclerosis patients, *J Neuroimmunol* **174** (2006), 108–118.

[17] W.I. McDonald, A. Compston, G. Edan, D. Goodkin, H.P. Hartung, F.D. Lublin, H.F. McFarland, D.W. Paty, C.H. Polman, S.C. Reingold, M. Sandberg-Wollheim, W. Sibley, A. Thompson, S. van den Noort, B.Y. Weinshenker and J.S. Wolinsky, Recommended diagnostic criteria for multiple sclerosis: guidelines from the international panel on the diagnosis of multiple sclerosis, *Ann Neurol* **50** (2001), 121–127.

[18] H. Sato, S. Ishida, K. Toda, R. Matsuda, Y. Hayashi, M. Shigetaka, M. Fukuda, Y. Wakamatsu and A. Itai A, New approaches to mechanism analysis for drug discovery using DNA microarray data combined with KeyMolnet, *Curr Drug Discov Technol* **2** (2005), 89–98.

[19] J. Satoh, Z. Illes, A. Peterfalvi, H. Tabunoki, C. Rozsa and T. Yamamura, Aberrant transcriptional regulatory network in T cells of multiple sclerosis, *Neurosci Lett* **422** (2007), 30–33.

[20] T. Kuzuhara, M. Suganuma, M. Kurusu and H. Fujiki, *Helicobacter pylori*-secreting protein Tipα is a potent inducer of chemokine gene expressions in stomach cancer cells, *J Cancer Res Clin Oncol* **133** (2007), 287–296.

[21] F. Rapaport, A. Zinovyev, M. Dutreix, E. Barillot E and J.P. Vert, Classification of microarray data using gene networks, *BMC Bioinformatics* **8** (2007), 35.

[22] P.J. Barnes and M. Karin, Nuclear factor-κB. A pivotal transcription factor in chronic inflammatory diseases, *N Engl J Med* **336** (1997), 1066–1071.

[23] Q. Li and I.M. Verma, NF-κB regulation in the immune system, *Nat Rev Immunol* **2** (2002), 725–734.

[24] H.L. Pahl, Activators and target genes of Rel/NF-κB transcription factors, *Oncogene* **18** (1999), 6853–6866.

[25] Y. Ben-Neriah, Regulatory functions of ubiquitination in the immune system, *Nat Immunol* **3** (2002), 20–26.

[26] D. Buljevac, W.C.J. Hop, W. Reedeker, A.C.J.W. Janssens, F.G.A. van der Meché, P.A. van Doorn and R.Q. Hintzen, Self reported stressful life events and exacerbations in multiple sclerosis: prospective study, *BMJ* **327** (2003), 646.

[27] W. Xiao, Advances in NF-κB signaling transduction and transcription, *Cell Mol Immunol* **1** (2004), 425–435.

[28] D. Gveric, C. Laltschmidt, M.L. Cuzner and J. Newcombe, Transcription factor NF-κB and inhibitor IκBα are localized in macrophages in active multiple sclerosis lesions, *J Neuropathol Exp Neurol* **57** (1998), 168–178.

[29] B. Bonetti, C. Stegagno, B. Cannella, N. Rizzuto, G. Moretto and C.S. Raine, Activation of NF-κB and c-*jun* transcription factors in multiple sclerosis lesions. Implications for oligodendrocyte pathology, *Am J Pathol* **155** (1999), 1433–1438.

[30] B. Miterski, S. Böhringer, W. Klein, E. Sindern, M. Haupts, S. Schimrigk and J.T. Epplen, Inhibitors in the NFκB cascade comprise prime candidate genes predisposing to multiple sclerosis, especially in selected combinations, *Genes Immun* **3** (2002), 211–219.

[31] B. Hilliard, E.B. Samoilova, T.S.T. Liu, A. Rostami and Y. Chen, Experimental autoimmune encephalomyelitis in NF-κB-deficient mice: roles of NF-κB in the activation and differentiation of autoreactive T cells, *J Immunol* **163** (1999), 2937–2943.

[32] K. Pahan and M. Schmid, Activation of nuclear factor-κB in the spinal cord of experimental allergic encephalomyelitis, *Neurosci Lett* **287** (2000), 17–20.

[33] G. van Loo, R. De Lorenzi, H. Schmidt, M. Huth, A. Mildner, M. Schmidt-Supprian, H. Lassman, M.R. Prinz and M. Pasparakis, Inhibition of transcription factor NF-κB in the central nervous system ameliorates autoimmune encephalomyelitis in mice, *Nat Immunol* **7** (2006), 954–961.

Neuropathology 2008; **28**, 561–576 doi:10.1111/j.1440-1789.2008.00915.x

Original Article

Neuromyelitis optica/Devic's disease: Gene expression profiling of brain lesions

Jun-ichi Satoh,[1,2] Shinya Obayashi,[2] Tamako Misawa,[2] Hiroko Tabunoki,[2] Takashi Yamamura,[1] Kunimasa Arima[3] and Hidehiko Konno[4]

[1]Department of Bioinformatics and Molecular Neuropathology, Meiji Pharmaceutical University, [2]Department of Immunology, National Institute of Neuroscience, NCNP, [3]Department of Laboratory Medicine, Musashi Hospital, NCNP, Tokyo, and [4]Department of Neurology, Nishitaga National Hospital, Sendai, Japan

Neuromyelitis optica (NMO), also known as Devic's disease, is an inflammatory demyelinating disease that affects selectively the optic nerves and the spinal cord, possibly mediated by an immune mechanism distinct from that of multiple sclerosis (MS). Recent studies indicate that NMO also involves the brain. Here, we studied gene expression profile of brain lesions of a patient with NMO by using DNA microarray, along with gene expression profile of the brains of Parkinson disease and amyotrophic lateral sclerosis patients. We identified more than 200 genes up-regulated in NMO brain lesions. The top 20 genes were composed of the molecules closely associated with immune regulation, among which marked up-regulation of interferon gamma-inducible protein 30 (IFI30), CD163, and secreted phosphoprotein 1 (SPP1, osteopontin) was validated by real time RT-PCR, Northern blot and Western blot analysis. Pathologically, CD68$^+$ macrophages and microglia expressed intense immunoreactivities for IFI30 and CD163 in NMO lesions, consisting of inflammatory demyelination, axonal loss, necrosis, cavity formation, and vascular fibrosis. KeyMolnet, a bioinformatics tool for analyzing molecular interaction on the curated knowledge database, suggested that the molecular network of up-regulated genes in NMO brain lesions involves transcriptional regulation by the nuclear factor-kappaB (NF-κB) and B-lymphocyte-induced maturation protein-1 (Blimp-1). These results suggest that profound activation of the macrophage-mediated proinflammatory immune mechanism plays a pivotal role in development of NMO brain lesions.

Correspondence: Jun-ichi Satoh, MD, Department of Bioinformatics and Molecular Neuropathology, Meiji Pharmaceutical University, 2-522-1 Noshio, Kiyose, Tokyo 204-8588, Japan. Email: satoj@my-pharm.ac.jp

Received 27 January 2008; revised and accepted 13 February 2008.

Key words: CD163, DNA microarray, IFI30, KeyMolnet, neuromyelitis optica.

INTRODUCTION

Neuromyelitis optica (NMO), also known as Devic's disease, is a severe inflammatory demyelinating disease that preferentially affects the optic nerves and the spinal cord in the human CNS.[1] The recently proposed diagnostic criteria for definite NMO requires optic neuritis and myelitis, and at least two of three supportive findings, including MRI evidence of a longitudinally extensive cord lesion, absence of multiple sclerosis (MS)-like brain lesions, or detection of the serum biomarker NMO-IgG that targets aquaporin-4 (AQP4), the most abundant water channel protein expressed in the CNS.[2] Pathologically, NMO lesions are characterized by extensive inflammatory demyelination and necrosis involving both the cortex and the white matter, associated with intense deposition of immunoglobulins and activated complement components around hyalinized blood vessels, and accompanied by accumulation of macrophages, granulocytes and eosinophils.[3] Furthermore, NMO lesions show a substantial loss of AQP4 and GFAP immunoreactivities, in contrast to enhanced expression of both in MS lesions.[4–6] These observations suggest that NMO constitutes a distinct disease entity, whose development is based primarily on a humoral mechanism, possibly different from the immune mechanism underlying MS, although a subtype of optic-spinal MS, accumulated in Asian countries, shows a considerable overlap with NMO.[1,7] Importantly, recent studies revealed that NMO frequently involves the brain, and brain MRI abnormalities do not exclude the clinical diagnosis of NMO.[8–13] At present, precise molecular events responsible for development of NMO lesions in the brain remain unknown.

Gene expression profiling by DNA microarray is an innovative technology that allows us to systematically monitor the expression of a large number of genes in disease-affected tissues. This approach has given new insights into the complexity of molecular interactions promoting the autoimmune process in MS.[14] The comprehensive gene expression profiling of MS brain tissues identified a battery of genes deregulated in MS, whose role has not been previously predicted in its pathogenesis.[15-17] Recently, we found that a battery of genes differentially expressed in $CD3^+$ T cells between untreated MS patients and healthy subjects were categorized into apoptosis signaling-related genes,[18] and T-cell gene expression profiling classifies a heterogeneous population of Japanese MS patients into four distinct subgroups that differ in the disease activity and therapeutic response to interferon-beta (IFNβ).[19] IFNβ immediately induces a burst of expression of chemokine genes with potential relevance to IFNβ-related early adverse effects in MS.[20]

In the present study, for the first time we investigated the gene expression profile of brain lesions of a patient with NMO by using DNA microarray technology. We have identified more than 200 genes up-regulated in NMO lesions. The immunohistochemical study and the molecular network analysis by a bioinformatics tool suggested that severe fulminant activation of the macrophage-mediated proinflammatory immune mechanism plays a pivotal role in development of NMO brain lesions.

MATERILAS AND METHODS

Human brain tissues

For microarray analysis, we prepared total RNA from a small block of autopsied frozen frontal lobe tissues that include both the cerebral cortex and the white matter. The brain tissues were isolated from a 70-year-old woman with neuromyelitis optica (NMO) who died of pneumonia, a 76-year-old woman with Parkinson disease (PD) who died of aspiration pneumonia, and a 61-year-old man with amyotrophic lateral sclerosis (ALS) who died of respiratory failure.

The patient with NMO developed weakness and dysesthesia of the left upper extremity at age 57 and left optic neuritis at age 60, and showed tetraparesis at age 62, was bedridden at age 67, and was affected with respiratory failure requiring tracheostomy at age 68. The CSF examination at age 62 showed mild pleocytosis with an increase in myelin basic protein (MBP) levels, but oligoclonal IgG bands (OCB) were undetectable. The neurological symptoms showed a relapsing-remitting clinical course. Intravenous methylprednisolone pulse (IVMP) was given at each event of acute relapse. Interferon-beta (IFNβ) was administered for four years from age 65 to age 70, although the last two weeks were completely free of IFNβ. The sagittal T2-weighted MRIs at age 63 identified a long discontinuous cervical cord lesion, and a follow-up study at age 67 showed marked atrophy of the entire cervical spinal cord (Fig. 1a,b). At 4 months before death, the patient developed sudden-onset visual loss and disturbed consciousness. The axial T2-weighted MRIs at the terminal stage showed multiple focal and diffuse extensive high-intensity lesions distributed predominantly in the deep cortical and periventricular white matter and brain stem regions (Fig. 1c,d). Since the patient's serum sample was not saved, immunoglobulin G (IgG) was isolated from the postmortem frozen brain tissues by using an IgG purification kit (Dojindo Laboratories, Kumamoto, Japan). The brain-derived IgG dissolved in PBS at the concentration of 0.73 μg/μL was processed for quantification of anti-AQP4 antibody according to the methods described previously.[21] This was found as positive at the titer of 8×, whereas IgG isolated from the brain tissues of the PD patient was negative for anti-AQP4 antibody (data not shown). Although there exists no gold standard for anti-AQP4 antibody levels in brain tissue-derived whole IgG preparation, we considered that the titer of 8× is significantly high, because anti-AQP4 antibody titers were usually much lower in the CSF than in the serum of NMO.[21] Thus, all of these observations supported the clinical diagnosis of NMO.

Only the brain was taken at autopsy in the NMO case, in which we dissected separately the cortex-enriched sample (NMO-C) and the white matter-enriched sample (NMO-W). The postmortem interval of the cases described above ranged from 2 to 3 h prior to freezing the brain tissues. Total RNA was extracted by homogenizing them in TRIZOL reagent (Invitrogen, Carlsbad, CA, USA). Pooled human frontal lobe total RNA (#636563, Clontech, Mountain View, CA, USA) was utilized as a control RNA that serves as the universal reference to standardize the gene expression levels in microarray analysis.

For immunohistochemistry, we prepared 10 micron-thick serial sections from the ipsilateral frontal lobe where microarray samples were taken or the corresponding contralateral frontal lobe of these cases. The tissue sections also included the frontal or parietal lobes of four MS cases, such as a 29-year-old woman with secondary progressive MS (SPMS) (MS#1), a 40-year-old woman with SPMS (MS#2), a 43-year-old woman with primary progressive MS (PPMS) (MS#3), and a 33-year-old man with SPMS (MS#4), and four neurologically normal cases, such as a 79-year-old woman who died of hepatic cancer (NNC#1), a 75 years-old woman who died of breast cancer (NNC#2), a 60 years-old woman who died of external auditory canal cancer (NNC#3), and a 74-year-old woman who died of gastric and hepatic cancers (NNC#4). The brain tissues

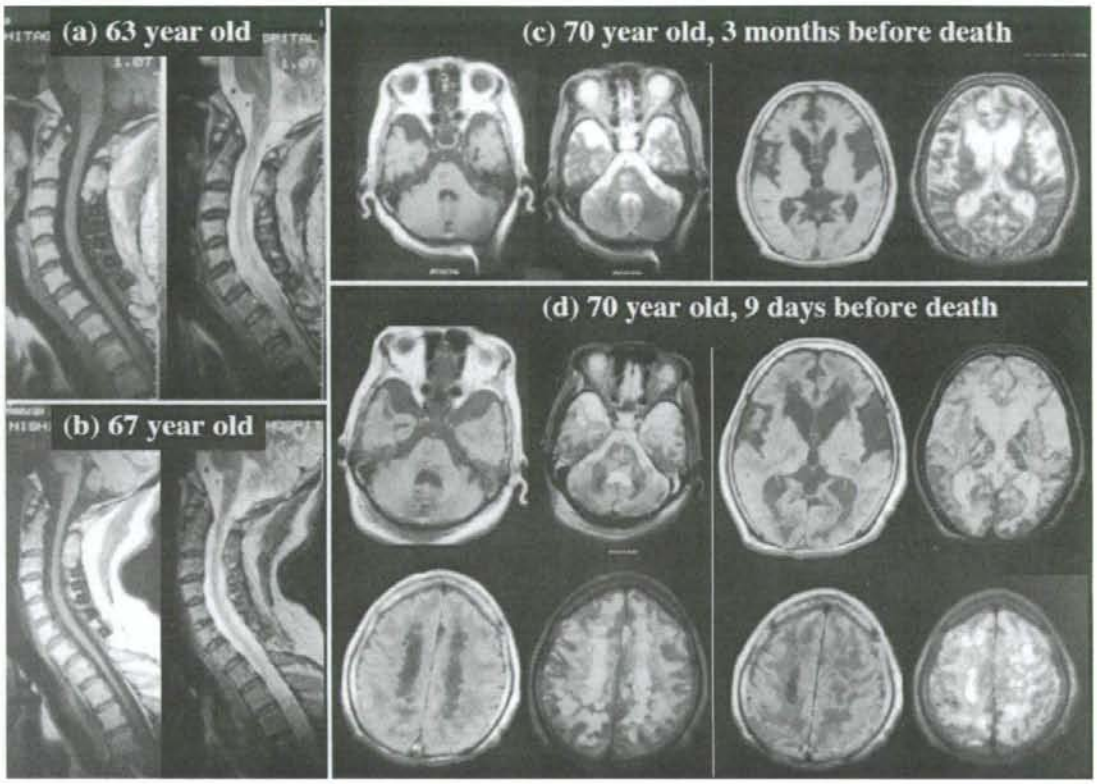

Fig. 1 MRI study of the neuromyelitis optica (NMO) patient. The patient developed the initial symptoms at age 57, followed by a relapsing-remitting clinical course, and died at age 70. (a) MRI of the cervical spinal cord at age 63, (b) MRI of the cervical spinal cord at age 67, (c) MRI of the brain at age 70 at 3 months before death, and (d) MRI of the brain at age 70 at 9 days before death. The left panels show T1-weighted images, while the right panels represent the corresponding T2-weighted images.

were fixed with 4% paraformaldehyde or 10% neutral formalin and embedded in paraffin.

All autopsies were performed either at the Musashi Hospital, National Center of Neurology and Psychiatry (NCNP), Tokyo, Japan or at the Nishitaga National Hospital, Sendai, Japan. Written informed consent was obtained regarding all the cases examined. The present study was approved by the Ethics Committee of NCNP.

DNA microarray analysis

We utilized a custom microarray containing duplicate spots of 1258 cDNA immobilized on a poly L-lysine-coated glass slide (Hitachi Life Science, Saitama, Japan).[18-20] The array includes a wide range of annotated genes, such as cytokines/growth factors and their receptors, apoptosis regulators, oncogenes, transcription factors, signal transducers, cell cycle regulators and housekeeping genes. Five μg of purified RNA was *in vitro* amplified, and the antisense RNA (aRNA) of the brain tissues was labeled with a fluorescent dye Cy5, while the universal reference RNA was labeled with Cy3. The arrays were hybridized at 62°C for 10 h in the hybridization buffer containing equal amounts of Cy3- or Cy5-labeled cDNA, and they were then scanned by the ScanArray 5000 scanner (GSI Lumonics, Boston, MA, USA). The data were analyzed by using the QuantArray software (GSI Lumonics). The average of fluorescence intensities (FI) of duplicate spots was obtained after global normalization between Cy3 and Cy5 signals. The gene expression level (GEL) was calculated according to the formula: GEL = FI (Cy5) of the sample/FI (Cy3) of the universal reference. The GEL ≥2.0 or <0.5 was considered as significant up-regulation or down-regulation.

Molecular network analysis

The molecular network of significant genes in microarray analysis was analyzed by using a bioinformatics tool named

KeyMolnet (Institute of Medicinal Molecular Design, Tokyo, Japan).[22] KeyMolnet constitutes a knowledge-based content database of numerous interactions among human genes, molecules, diseases, pathways and drugs. They have been manually collected and carefully curated from selected review articles, literature, and public databases by expert biologists of IMMD. The KeyMolnet contents, composed of approximately 12 000 molecules, are focused on human species, and categorized into either the core contents collected from selected review articles or the secondary contents extracted from abstracts of the PubMed database.

When the list of Entrez gene ID of the genes extracted from microarray data was imported into KeyMolnet, it automatically provided corresponding molecules as a node on networks.[23] Among four different modes of the molecular network search, the "common upstream" search makes it possible to extract the most relevant molecular network composed of the genes coordinately regulated by putative "common upstream" transcription factors. The extracted molecular network was compared side by side with 346 distinct human canonical pathways of the KeyMolnet library. They include a broad range of signal transduction pathways, metabolic pathways, and transcriptional regulatory pathways. The statistical significance in concordance between the extracted network and the canonical pathway was evaluated by the algorithm that counts the number of overlapping molecular relations between both. This makes it possible to identify the canonical pathway showing the most significant contribution to the extracted network. The calculation of significance score is based on the following formula, where O = the number of overlapping molecular relations between the extracted network and the canonical pathway, V = the number of molecular relations located in the extracted network, C = the number of molecular relations located in the canonical pathway, T = the number of total molecular relations installed in KeyMolnet, and X = the sigma variable that defines coincidence.

$$\text{Score} = -\log_2(\text{Score}\,(P))$$

$$\text{Score}\,(P) = \sum_{x=O}^{Min(C,\,V)} f(x)$$

$$f(x) = {}_{C}C_{x} \cdot {}_{T-C}C_{V-x} / {}_{T}C_{V}$$

Immunohistochemistry

After deparaffination, the tissue sections were heated in 10 mM citrate sodium buffer, pH 6.0 by autoclave at 125°C for 30 s in a temperature-controlled pressure chamber (Dako, Tokyo, Japan). They were treated at room temperature (RT) for 15 min with 3% hydrogen peroxide-containing methanol to block the endogenous peroxidase activity. The tissue sections were then incubated with PBS containing 10% normal rabbit serum or 10% normal goat serum at RT for 15 min to block non-specific staining. The serial sections were incubated in a moist chamber at 4°C overnight with primary antibodies listed in Table 1, as described previously.[24] After washing with PBS, the tissue sections were labeled at RT for 30 min with horseradish peroxidase (HRP)-conjugated secondary antibodies (Nichirei, Tokyo, Japan), followed by incubation with a colorizing solution containing diaminobenzidine tetrahydrochloride (DAB) and a counterstain with hematoxylin. For negative controls, the step of incubation with primary antibodies was omitted.

Western blot analysis

To prepare total protein extract, frozen brain tissues were homogenized in radio-immunoprecipitation assay (RIPA) lysis buffer composed of 50 mM Tris-HCl, pH 7.5, 150 mM NaCl, 1% Nonidet P40, 0.5% sodium deoxycholate, 0.1% SDS, and a cocktail of protease inhibitors (Roche Diagnositics, Tokyo, Japan), followed by centrifugation at 13 400 *g* for 20 min. The supernatant was collected for separation on a 12% SDS-PAGE gel. The protein concentration was determined by a Bradford assay kit (Bio-Rad, Hercules, CA, USA). After gel electrophoresis, the protein was transferred onto nitrocellulose membranes, and immunolabeled at RT overnight with primary antibodies listed in Table 1, as described previously.[24] Then, the membranes were incubated at RT for 30 min with HRP-conjugated antimouse or goat IgG (Santa Cruz Biotechnology, Santa Cruz, CA, USA). The specific reaction was visualized by using a chemiluminescent substrate (Pierce, Rockford, IL, USA). After the antibodies were stripped by incubating the membranes at 50°C for 30 min in stripping buffer composed of 62.5 mM Tris-HCl, pH 6.7, 2% SDS and 100 mM 2-mercaptoethanol, the membranes were processed for relabeling several times with different antibodies.

Real-time RT-PCR analysis

DNase-treated total RNA was processed for cDNA synthesis using oligo(dT)$_{12-18}$ primers and SuperScript II reverse transcriptase (Invitrogen, Carlsbad, CA, US). Then, cDNA was amplified by PCR in LightCycler ST300 (Roche Diagnostics, Tokyo, Japan) using ®SYBR Green I and the following sense and antisense primer sets; 5′ctcag gagtgtttgcttcaagtgg3′ and 5′tagcaccattcttagtggagcagg3′ for interferon gamma-inducible protein 30 (IFI30), 5′gacgat gctcaggtggtgtgtcaa3′ and 5′tccttgtgcccacaccactcactatgg3′ for CD163, and 5′gaagatatgctggttgtagacccc3′ and 5′acagg gagtttccatgaagccac3′ for secreted phosphoprotein 1 (SPP1). The levels of expression of target genes were quantified by standardizing them against those of the

Table 1 Primary antibodies utilized for immunochemistry and Western blot analysis

Antibodies (name)	Suppliers	Code	Origin	Immunogens	Antigen specificity	Concentration used for immunohistochemistry	Concentration used for Western blotting
GFAP	Dako	N1506	Rabbit	Purified bovine spinal cord GFAP	GFAP	Prediluted	NA
MBP	Dako	N1564	Rabbit	Purified human brain MBP	MBP	Prediluted	NA
NF (2F11)	Nichirei	412551	Mouse	Purified human brain NF protein	Human 70-kDa and 200-kDa NF	Prediluted	NA
CD68 (KP1)	Dako	N1577	Mouse	Lysosomal granules of human lung macrophages	CD68	Prediluted	NA
CD3 (PS1)	Nichirei	413241	Mouse	Recombinant human CD3 epsilon chain	CD3	Prediluted	NA
CD163 (10D6)	Novocastra	NCL-CD163	Mouse	Recombinant human CD163 corresponding to domains of 1–4 of the N-terminal region	CD163	1:50 of the hybridoma cuture supernatant	1:250 of the hybridoma culture supernatant
IFI30 (T-18)	Santa Cruz Biotechnology	sc-21827	Goat	A peptide mapping within an internal region of human IFI30 (GILT)	IFI30	1:500 (400 ng/mL)	1:1000 (200 ng/mL)
AQP4 (H-80)	Santa Cruz Biotechnology	sc-20812	Rabbit	Amino acid residues 244–323 mapping at the C-terminus of human AQP4	AQP4	1:250 (800 ng/mL)	NA
AQP1 (H-55)	Santa Cruz Biotechnology	sc-20810	Rabbit	Amino acid residues 215–269 of human AQP1	AQP1	1:250 (800 ng/mL)	NA
HSP60 (N-20)	Santa Cruz Biotechnology	sc-1052	Goat	A peptide mapping at the amino terminus of human HSP60	HSP60	NA	1:2000 (100 ng/mL)

AQP1, aquaporin-1; AQP4, aquaporin-4; HSP60, 60-kDa heat shock protein; IFI30, interferon gamma-inducible protein 30; NA, not applied; NF, neurofilament.

glyceraldehyde-3-phosphate dehydrogenase (G3PDH) gene detected in the identical cDNA samples by using the primer set of 5'ccatgttcgtcatgggtgtgaacca3' and 5'gccagta gaggcagggatgatgttc3', as described previously.[25] All the assays were performed in triplicate.

Northern blot analysis

Three μg of total RNA was separated on a 1.5% agarose–6% formaldehyde gel and transferred onto a nylon membrane, as described previously.[18] After prehybridization, the membranes were hybridized at 54°C overnight with the digoxigenin (DIG)-labeled DNA probe synthesized by the PCR DIG probe synthesis kit (Roche Diagnositics) using the sense and antisense primer sets described above. The specific reaction was visualized on Kodak X-OMAT AR X-ray films by the DIG chemiluminescence detection kit (Roche Diagnositics).

RESULTS

Gene expression profile of NMO, PD and ALS brain tissues

First, we investigated the gene expression profile of the frontal lobe brain tissues, including the cortex-enriched sample of NMO (NMO-C), the white matter-enriched sample of NMO (NMO-W), and the whole brain of PD and ALS, by analyzing a cDNA microarray of 1258 genes. When compared with the gene expression levels in the pooled human frontal lobe total RNA as the universal reference, the number of up-regulated genes was 225, 234, 31 or 20, whereas that of down-regulated genes was 173, 158, 71 or 64 in the brains of NMO-C, NMO-W, PD or ALS, respectively (Table 2). The great majority (16 genes, 80%) of top 20 genes were common between NMO-C and NMO-W, supporting the reproducibility of microarray experiments. Top 20 genes were composed of the molecules closely associated with immune regulation, such as chemokines/cytokines and the receptors, including chemokine C-C motif ligand 18 (CCL18), chemokine C-C motif ligand 20 (CCL20), chemokine C-X-C motif ligand 5 (CXCL5), chemokine C-X-C motif receptor 4 (CXCR4), interleukin 6 (IL6) and interleukin 10 receptor alpha (IL10RA), and the cell-surface accessory molecules, including major histocompatibility complex class II antigens HLA-DRA, HLA-DRB1, HLA-DRB5, Fc fragment of IgE receptor FCER1G, Fc fragment of IgG receptor FCGR2B and CD86. Among top 20 genes, interferon gamma-inducible protein 30 (IFI30) with a 66-fold or 56-fold increase, CD163 with a 62-fold or 79-fold increase, and secreted phosphoprotein 1 (SPP1, alternatively named osteopontin) with a 61-fold or 95-fold increase were listed as top 3 markedly up-regulated genes in both NMO-C and NMO-W.

In contrast, the gene expression profile of PD and ALS brains was fairly different from the profile of NMO. The expression of several glutathione S-transferases, including GSTM1 and GSTM2, an antioxidant marker, was moderately elevated in PD and ALS brains (Table 2), whereas the levels of GSTM1 and GSTM2 were not elevated in NMO brains (data not shown). The expression of insulin-like growth factor 2 (IGF2) and IGF-binding protein 2 (IGFBP2) was elevated in PD brain, and the levels of proenkephalin (PENK) and fibroblast growth factor 9 (FGF9) were increased in ALS brain (Table 2). On the contrary, the level of expression of IGF2 and IGFBP2 were not elevated, and the expression of PENK and FGF9 was decreased in NMO brains (data not shown).

Validation of microarray data

The microarray experiments indicated remarkable up-regulation of IFI30, CD163 and SPP1 in both NMO-C and NMO-W. In the next step, we verified these observations by Northern blot analysis (Fig. 2A, panels a–c, lanes 2 and 3), real-time RT-PCR analysis (Fig. 2B, panels a–c), and Western blot analysis (Fig. 2C, panels a and b, lanes 1 and 2). Thus, microarray data correlated well with the data of three distinct modes of expression analysis described above.

Molecular network of up-regulated genes in NMO brains

Since microarray analysis produced a large amount of gene expression data, it is often difficult to find out the meaningful relationship between gene expression profile and biological implications from such a large quantity of available data. To overcome this difficulty, we have made a breakthrough to identify the molecular network most closely associated with DNA microarray data by using KeyMolnet, a bioinformatics tool for analyzing molecular interaction on the curated knowledge database. When the list of Gene ID of 234 genes up-regulated in NMO-W was imported into KeyMolnet, it extracted 413 molecules directly linked to 234 genes. Subsequently, the common upstream search of 413 molecules generated a complex network composed of 418 fundamental nodes and 1326 molecular relations (Fig. 3). The statistical evaluation of the extracted network showed the most signficant relationship with transcriptional regulation by the nuclear factor-kappaB (NF-κB) at the first rank where the score was 18.3 and the score (P) = 3.019E-006, followed by B-lymphocyte-induced maturation protein-1 (Blimp-1) at the second rank where the score was 17.6 and the score (P) = 4.874E-006,

Table 2 Top 20 up-regulated genes in the brains of neuromyelitis optica (NMO), Parkinson diseases (PD) and amyotrophic lateral sclerosis (ALS)

Disease	NMO-C			NMO-W			PD			ALS		
Rank	GEL	Symbol	Name	GEL	Symbol	Name	GEL	Symbol	Name	GEL	Symbol	Name
1	66.29	IFI30	Interferon, gamma-Inducible protein 30	95.43	SPP1	Secreted phosphoprotein 1 (osteopontin, bone sialoprotein I, early T-lymphocyte activation 1)	3.65	GSTM1	Glutathione S-transferase M1	3.79	GSTA2	Glutathione S-transferase A2
2	62.21	CD163	CD163 molecule	79.38	CD163	CD163 molecule	3.30	IGFBP2	Insulin-like growth factor binding protein2, 36*TH* kDa	3.24	PENK	Proenkephalin
3	61.39	SPP1	Secreted phosphoprotein 1 (osteopontin, bone sialoprotein I, early T-lymphocyte activation 1)	55.78	IFI30	Interferon, gammainducible protein 30	3.18	TNFRSF11B	Tumor necrosis factor receptor superfamily, member 11b (osteoprotegerin)	2.40	RBBP6	Retinoblastoma binding protein 6
4	37.30	CXCR4	Chemokine (C-X-C motif) receptor 4	39.69	FCER1G	Fc fragment of IgE, high affinity I, receptor for; gamma polypeptide	3.15	PRODH	Proline dehydrogenase (oxidase) 1	2.38	COX4I1	Cytochrome c oxidase subunit IV isoform 1
5	37.09	FCER1G	Fc fragment of IgE, high affinity I, receptor for; gamma polypeptide	37.07	HLA-DRA	Major histocompatibility complex, class II, DR alpha	3.07	CXCL2	Chemokine (C-X-C motif) ligand 2	2.34	RASSF7	Ras association (RalGDS/AF-6) domain family 7
6	36.65	HLA-DRA	Major histocompatibility complex, class II, DR alpha	35.97	CXCR4	Chemokine (C-X-C motif) receptor 4	2.98	DUSP1	Dual specificity phosphatase 1	2.31	COX7A1	Cytochrome c oxidase subunit VIIa polypeptide 1 (muscle)
7	26.91	FCGR2B	Fc fragment of IgG, low affinity IIb, receptor (CD32)	33.09	FCGR2B	Fc fragment of IgG, low affinity IIb, receptor (CD32)	2.98	IGF2	Insulin-like growth factor 2 (somatomedin A)	2.28	GSTT2	Glutathione S-transferase theta 2
8	23.80	HSPB7	Heat shock 27*TH* kDa protein family, member 7 (cardiovascular)	31.38	CCL20	Chemokine (C-C motif) ligand 20	2.93	HSPB1	Heat shock 27*TH* kDa protein 1	2.27	GSTZ1	Glutathione transferase zeta 1 (maleylacetoacetate isomerase)
9	23.07	CCL20	Chemokine (C-C motif) ligand 20	30.66	CCL18	Chemokine (C-C motif) ligand 18 (pulmonary and activation-regulated)	2.92	ADH1A	Alcohol dehydrogenase 1A (class I), alpha polypeptide	2.18	NFKBIA	Nuclear factor of kappa light polypeptide gene enhancer in B-cells inhibitor, alpha
10	22.20	HLADRB5	Major histocompatibility complex, class II, DR beta 5	25.51	HLADRB5	Major histocompatibility complex, class II, DR beta 5	2.70	GSTM2	Glutathione S-transferase M2 (muscle)	2.17	GSTM1	Glutathione S-transferase M1
11	19.88	HLADRB1	Major histocompatibility complex, class II, DR beta 1	19.54	HLADRB1	Major histocompatibility complex, class II, DR beta 1	2.70	RAB13	RAB13, member RAS oncogene family	2.16	GJB1	Gap junction protein, beta 1, 32*TH* kDa
12	19.01	CXCL5	Chemokine (C-X-C motif) ligand 5	16.70	IL10RA	Interleukin 10 receptor, alpha	2.66	TRAF4	TNF receptorassociated factor 4	2.15	RHOG	Ras homolog gene family, member G (rho G)
13	18.82	IL10RA	Interleukin 10 receptor, alpha	16.69	CD86	CD86 molecule	2.65	CXCL1	Chemokine (C-X-C motif) ligand 1 (melanoma growth stimulating activity, alpha)	2.14	CXCL14	Chemokine (C-X-C motif) ligand 14